

First analysis of GLE 72 event on 10 September 2017: Spectral and anisotropy characteristics

A.L. Mishev¹, I.G. Usoskin^{1,2}, O. Raukunen³, M. Paassilta³, E. Valtonen³, L.G. Kocharov², and R. Vainio³

¹Space Climate Research Unit, University of Oulu, Finland.

²Sodankylä Geophysical Observatory, University of Oulu, Finland.

³Department of Physics and Astronomy, University of Turku, Finland.

October 24, 2018

Abstract

Using neutron monitor and space-borne data we performed an analysis of the second ground level enhancement of solar cycle 24, namely the event of 10 September 2017 (GLE 72) and derive the spectral and angular characteristics of GLE particles. We employ new neutron monitor yield function and a recently proposed model based on optimization procedure. The method consists of simulation of particle propagation in a model magnetosphere in order to derive the cut-off rigidity and neutron monitor asymptotic directions. Subsequently the rigidity spectrum and anisotropy of GLE particles are obtained in their dynamical evolution during the event on the basis of inverse problem solution. The derived angular distribution and spectra are briefly discussed.

Keywords: Solar eruptive events, Ground level enhancement, Neutron Monitor

For contact: alexander.mishev@oulu.fi

1 Introduction

A detailed study of solar energetic particle (SEP) events provides important basis to understand their acceleration and propagation in the interplanetary space (Debrunner *et al.*, 1988; Lockwood, Debrunner, and Flückiger, 1990; Kallenrode, Cliver, and Wibberenz, 1992; Reames, 1999; Drake *et al.*, 2009; Tylka and Dietrich, 2009; Li *et al.*, 2012; Vainio *et al.*, 2013; Gopalswamy *et al.*, 2014; Kocharov *et al.*, 2017; Vainio *et al.*, 2017). Energetic and sporadic solar flares and coronal mass ejections (CMEs) can produce solar energetic particles (e.g. Reames, 1999; Cliver, Kahler, and Reames, 2004; Aschwanden, 2012; Reames, 2013; Desai and Giacalone, 2016, and references therein). Normally the maximum energy of SEPs is several MeV/nucleon, rarely exceeding 100 MeV/nucleon. However, in some cases the SEP energy reaches several GeV/nucleon.

While lower energy SEPs are absorbed in the atmosphere, those with energy above 300-400 MeV/nucleon generate an atmospheric shower, namely a complicated nuclear-electromagnetic-muon cascade consisting of large amount of secondary particles, which can reach the ground and eventually registered by ground based detectors, e.g. neutron monitors (NMs). The probability of occurrence of a high-energy SEP event is larger during the maximum and declining phase of the solar activity cycle (e.g. Shea and Smart, 1990). This particular class of events is known as ground level enhancements (GLEs).

Such events can be conveniently studied using the worldwide NM network, a multi-instrumental equipment for continuous monitoring of the intensity of cosmic ray (CR) particles and registration of GLEs (Simpson, Fonger, and Treiman, 1953; Hatton, 1971; Bieber and Evenson, 1995; Stoker, Dorman, and Clem, 2000; Mavromichalaki *et al.*, 2011; Gopalswamy *et al.*, 2012; Moraal and McCracken, 2012; Papaioannou *et al.*, 2014; Gopalswamy *et al.*, 2014). The distribution of NMs at different geographic regions allows one to obtain an exhaustive record of cosmic rays in space, because their intensity is not uniform in the vicinity of Earth (Bieber and Evenson, 1995; Mavromichalaki *et al.*, 2011). This fact plays an important role for GLE analysis, since an essential anisotropic part, normally during the event's onset is observed (Vashenyuk *et al.*, 2006; Bütikofer *et al.*, 2009; Mishev and Usoskin, 2016a). The full list of NMs used for the analysis of GLE 72 on 10 September 2017, with the corresponding abbreviations, cut-off rigidities and altitudes is given in Table 1.

Table 1: Neutron monitors with corresponding cut-off rigidities, geographic coordinates and altitudes above the sea level used for the analysis of GLE 72.

Station	latitude [deg]	Longitude [deg]	P_c [GV]	Altitude [m]
Alma Aty (AATY)	43.25	76.92	6.67	3340
Apatity (APTY)	67.55	33.33	0.48	177
Athens (ATHN)	37.98	23.78	8.42	260
Baksan (BKSN)	43.28	42.69	5.6	1700
Dome C (DOMC)	-75.06	123.20	0.1	3233
Dourbes (DRBS)	50.1	4.6	3.34	225
Fort Smith (FSMT)	60.02	248.07	0.25	0
Inuvik (INVK)	68.35	226.28	0.16	21
Irkutsk (IRKT)	52.58	104.02	3.23	435
Jang Bogo(JNBG)	-74.37	164.13	0.1	29
Jungfraujoeh (JUNG)	46.55	7.98	4.46	3476
Kerguelen (KERG)	-49.35	70.25	1.01	33
Lomnický štít (LMKS)	49.2	20.22	3.72	2634
Magadan (MGDN)	60.12	151.02	1.84	220
Mawson (MWSN)	-67.6	62.88	0.22	0
Mexico city (MXCO)	19.33	260.8	7.59	2274
Moscow (MOSC)	55.47	37.32	2.13	200
Nain (NAIN)	56.55	298.32	0.28	0
Newark (NWRK)	39.70	284.30	1.97	50
Oulu (OULU)	65.05	25.47	0.69	15
Peawanuck (PWNK)	54.98	274.56	0.16	52
Potchefstroom (PTFM)	-26.7	27.09	6.98	1351
Rome (ROME)	41.9	12.52	6.11	60
South Pole (SOPO)	-90.00	0.0	0.01	2820
Terre Adelie (TERA)	-66.67	140.02	0	45
Thule (THUL)	76.60	291.2	0.1	260
Tixie Bay (TXBY)	71.60	128.90	0.53	0

The first ten days of September 2017 were characterized by intense solar activity. During this period several X-class flares and CMEs were produced. The GLE 72 on 10 September 2017 event was related to a X8.2 solar flare, a climax on a series of flares from active region 12673. It peaked at 16:06 UT, leading to a gradual solar energetic particle event measured by spacecraft up to proton energies exceeding 700 MeV/n (Fig. 1), and to a very fast CME erupting over the west limb (Fig. 2). The CME was first observed in SOHO / LASCO / C2 field of view at 16:00:07 UT. The initial speed of the CME was very high, 3620 km s^{-1} , as measured from the leading edge of the structure at position angle 270° , i.e., to the west. The CME drove a shock front through

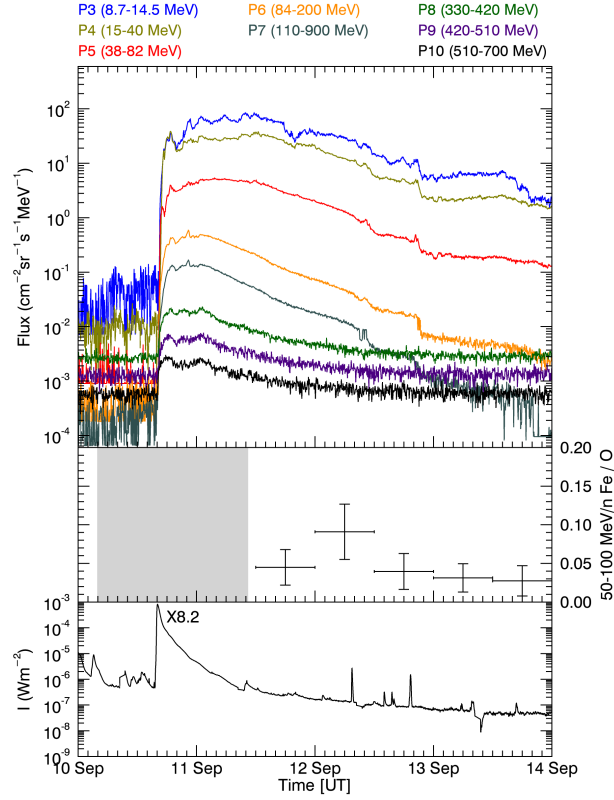


Figure 1: The 2017-09-10 SEP event and the related gradual soft X-ray flare as observed by GOES and SOHO / ERNE. The top panel shows the proton fluxes measured by GOES, the middle panel shows the Fe/O ratio at 50–100 MeV/n measured by SOHO / ERNE and the bottom panel shows the soft X-ray intensity measured by GOES. Note that SOHO / ERNE had a data gap in the beginning of the SEP event, indicated by the gray area in the respective panel.

the corona, with the flanks being traced in the atmospheric imaging assembly (AIA) of the Solar Dynamics Observatory (SDO) spacecraft image and the nose visible as a fainter structure in front of the brightest part of the CME.

The GLE onset was observed by several NM stations at about 16:15 UT (e.g. FSMT and INVK with statistically significant increase) and the corresponding alert signal was revealed after 17:00 (Souvatzoglou *et al.*, 2014). However, a statistically significant and high enough signal, which allows one to derive the spectral and angular characteristics of SEPs with sufficient precision, was observed at 16:30 UT (see Sections 2 and 3). The strongest NM increases were observed at the DOMC/DOMB ($\approx 10\text{--}15\%$, Fig. 3a), SOPO/SOPB ($\approx 5\text{--}8\%$, Fig. 3a) and FSMT ($\approx 6\%$, Fig. 3f) compared to the pre-increase levels, see details in Fig. 3. The count rate increase at FSMT was steeper compared to other stations, which recorded gradual increases. Herein DOMB, accordingly SOPB correspond to the lead free NMs at Dome C and South Pole stations, respectively. The event was characterized by a typical gradual increase, relatively hard rigidity spectrum and strong to moderate anisotropy during the event onset, which rapidly decreases resulting in a nearly isotropic flux. Similarly to some other events, it occurred during the recovery phase of a Forbush decrease, which is explicitly considered in our analysis. The background due to GCR is

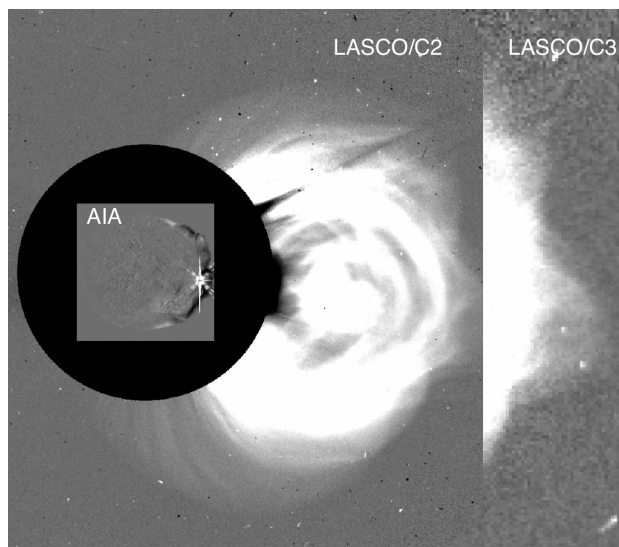


Figure 2: The 2017-09-10T16:00:07 CME as observed by SOHO / LASCO and SDO / AIA. The observation times of AIA and LASCO/C2 are 16:12:08 and 16:12:48, respectively. AIA observations are shown in 24-minute running differencing and the LASCO observations in 12-minute (or the best possible) running difference imaging. The C3 image shows the CME only 6 minutes later than the C2 image, indicating how exceptionally fast the CME was. All frames are centered in the same way and have the same scale. The image was created using Helioviewer (www.helioviewer.org).

averaged over two hours before the event’s onset, therefore we accounted for the corresponding variations of each NM count rates for exact computation of the background. Herein, we perform an analysis of this event using 5-min integrated NM data retrieved from neutron monitor data base NMDB (<http://www.nmdb.eu/>) (e.g. Mavromichalaki *et al.*, 2011), available also at the international GLE database (<http://gle.oulu.fi/#/>).

2 Modelling the neutron monitor response

In this study we employ a method similar to (Shea and Smart, 1982; Humble *et al.*, 1991; Cramp *et al.*, 1997; Bombardieri *et al.*, 2006; Vashenyuk *et al.*, 2006, 2008). The detailed description of the method is given elsewhere (Mishev, Kocharov, and Usoskin, 2014; Mishev and Usoskin, 2016a; Mishev, Usoskin, and Kocharov, 2017; Mishev, Poluianov, and Usoskin, 2017). The method implies modelling of NM response using an initial guess similarly to Mishev and Usoskin (2016b); Kocharov *et al.* (2017), and/or to Cramp, Humble, and Duldig (1995) and optimization procedure over a selected space of unknowns describing SEP characteristics. Note, that for a good convergence of the optimization we need about $2(n - 1)$ NM stations with non-null response, where n is the number of unknowns (e.g. Himmelblau, 1972). However, our method allows to derive a robust solution even in the case of relatively weak recorded NM increases on the basis of a specific numeric procedure, namely using a variable regularization (e.g. Tikhonov *et al.*, 1995; Mishev, Poluianov, and Usoskin, 2017).

Herein, we used a newly computed NM yield function, which is in a good agreement with

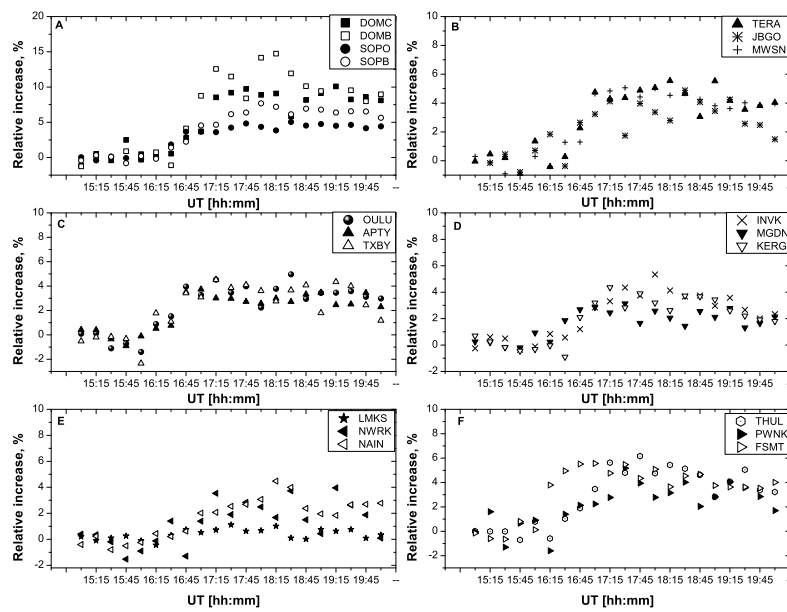


Figure 3: Count rate variation of NMs with statistically significant increase during GLE 72 on 10 September 2017.

experiments and recent modelling (Mishev, Usoskin, and Kovaltsov, 2013; Gil *et al.*, 2015; Mangeard *et al.*, 2016). We reduce model eventual uncertainties related to normalization of high-altitude NMs to sea level by employing yield function corresponding to the proper altitude of NMs above sea level (Mishev, Usoskin, and Kovaltsov, 2015) and appropriate scaling of mini NM to a standard 6NM64 (Caballero-Lopez, 2016; Lara, Borgazzi, and Caballero-Lopez, 2016).

In our model we can use as an approximation a modified power law or an exponential rigidity spectrum similarly to Cramp *et al.* (1997); Vashenyuk *et al.* (2008). The rigidity spectrum of SEPs described by a modified power is given by the expression:

$$J_{\parallel}(P) = J_0 P^{-(\gamma + \delta\gamma(P-1))} \quad (1)$$

where $J_{\parallel}(P)$ denotes the flux of particles with rigidity P , which arrive from the Sun along the axis of symmetry identified by geographic latitude Ψ and longitude Λ . The spectrum is described by γ - power-law spectral exponent and the rate of the spectrum steepening $\delta\gamma$.

Accordingly, the exponential rigidity spectrum is given by:

$$J_{\parallel}(P) = J_0 \exp(-P/P_0). \quad (2)$$

where P_0 is a characteristic proton rigidity.

The pitch angle distribution in all cases is modelled as superposition of two Gaussians:

$$G(\alpha(P)) \sim \exp(-\alpha^2/\sigma_1^2) + B \cdot \exp(-(\alpha - \pi)^2/\sigma_2^2) \quad (3)$$

where α is the pitch angle, σ_1 and σ_2 quantify the width of the pitch angle distribution, B describes the amount of particle flux arriving from the anti-sun direction. This allows us to consider a bidirectional particle flow.

The optimization is performed by minimizing the squared sum of difference between the modelled and measured NM responses employing the Levenberg-Marquardt method (Levenberg, 1944; Marquardt, 1963) with variable regularization (Tikhonov *et al.*, 1995), similarly to Mavrodiev, Mishev, and Stamenov (2004). We assess the goodness of the fit on the basis of several criteria. The general criterion \mathcal{D} , i.e. the residual (Equation 4) is according to (e.g. Himmelblau, 1972; Dennis and Schnabel, 1996).

$$\mathcal{D} = \frac{\sqrt{\sum_{i=1}^m \left[\left(\frac{\Delta N_i}{N_i} \right)_{mod.} - \left(\frac{\Delta N_i}{N_i} \right)_{meas.} \right]^2}}{\sum_{i=1}^m \left(\frac{\Delta N_i}{N_i} \right)_{meas.}} \quad (4)$$

According to our experience a good convergence of the optimization process and a robust solution are reached for $\mathcal{D} \leq 5\%$ similarly to Vashenyuk *et al.* (2006); Mishev and Usoskin (2016a). Normally \mathcal{D} is roughly 5% for strong events and $\sim 10\text{--}15\%$ for weak events such as GLE 72 (e.g. Mishev, Usoskin, and Kocharov, 2017; Mishev, Poluianov, and Usoskin, 2017). Therefore, we use additional criteria, namely the relative difference between the observed and calculated relative NM count rate increase should be about 10–20% for each station and the residuals should have a nearly-symmetric distribution, viz. the number of NMs under and/or over estimating the count rate must be roughly equal (e.g. Himmelblau, 1972).

The modelling of SEPs propagation in the geomagnetosphere used for computation of the cut-off rigidities and asymptotic directions of NMs (Cooke *et al.*, 1991) is performed with the

MAGNETOCOSMICS code (Desorgher *et al.*, 2005), using International Geomagnetic Reference Field (IGRF) geomagnetic model (epoch 2015) as the internal field model (Langel, 1987) and the Tsyganenko 89 model as the external field (Tsyganenko, 1989). This combination provides straightforward and precise modelling of SEPs propagation in the Earth’s magnetosphere (Kudela and Usoskin, 2004; Kudela, Bučik, and Bobik, 2008; Nevalainen, Usoskin, and Mishev, 2013).

3 Results of the analysis

We studied different cases, assumed in our model, of spectral and PAD functional shapes, namely modified power law or exponential rigidity spectra of SEPs, single or double Gaussian PAD, which encompass all the possibilities in the model (Equations 2–4). An example of several computed asymptotic directions used for GLE 72 analysis is presented in Figure 4. Here we plot the asymptotic directions in the rigidity range from 1 to 5 GV (for DOMC and SOPO respectively from 0.7 to 5 GV) in order to show the range of maximal NM response, while in the analysis we used the range between the lower rigidity cut-off of the station P_{cut} , i.e. the rigidity of the last allowed trajectory, below which all trajectories are forbidden, and the maximal assumed rigidity of SEPs being 20 GV.

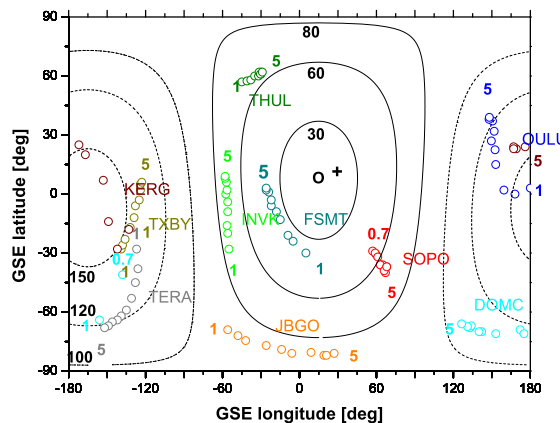


Figure 4: Asymptotic directions of several NM stations during the GLE 72 event on 10 September 2017 at 16:45 UT. The color lines and numbers indicate the NM stations and asymptotic directions (abbreviations given in Table 1). The small oval depicts the derived apparent source position, while the cross the IMF according to ACE satellite measurements. The lines of equal pitch angles relative to the derived anisotropy axis are plotted for 30°, 60°, 80° for sunward directions (solid lines), 100°, 120° and 150°, for anti-Sun direction (dashed lines).

The best fit is obtained assuming a modified power law rigidity spectra of SEPs and double Gaussian PAD (see below). For illustration we plot results with similar fit quality \mathcal{D} . The derived rigidity spectra of the high-energy SEPs during different stages of the event are presented in Figure 5, assuming a power law rigidity spectrum and a wide PAD fitted with a double Gaussian (Equations 1 and 3).

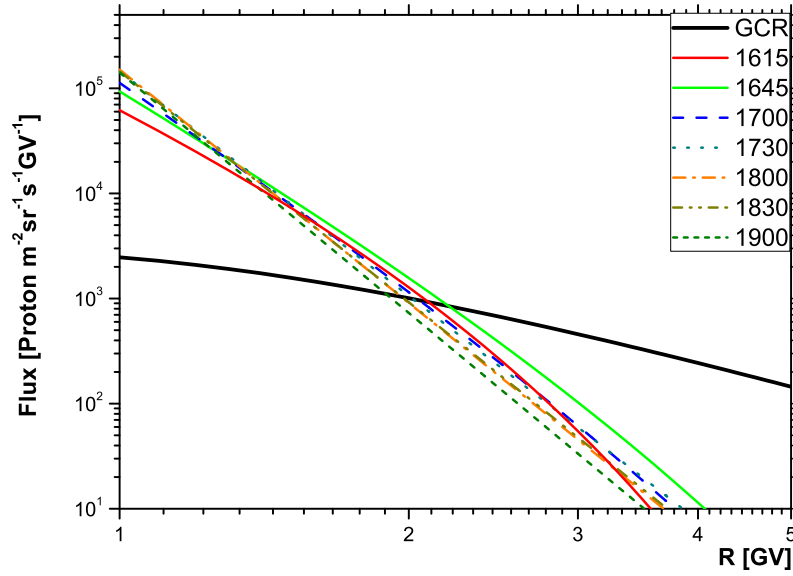


Figure 5: Derived SEP rigidity spectra during GLE 72 on 10 September 2017. The black solid line denotes the GCR particle flux, which corresponds to the time period of the GLE 72 occurrence and includes protons and α -particles, the latter representative also for heavy nuclei. Time (UT) corresponds to the start of the five minute interval over which the data are integrated.

The corresponding pitch angle distributions assuming a double Gaussian PAD are presented in Figure 6.

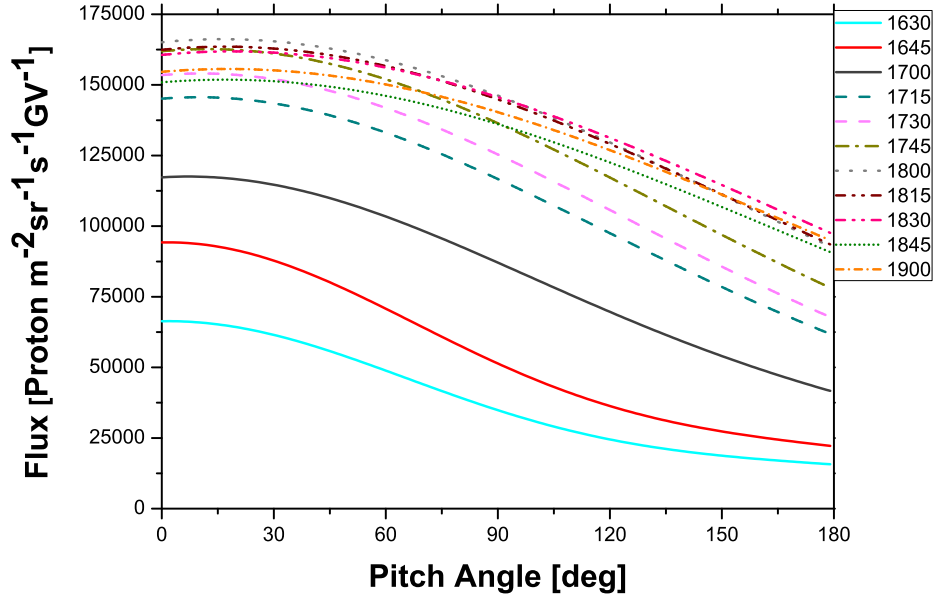


Figure 6: Derived PAD during GLE 72 on 10 September 2017. Time (UT) corresponds to the start of the five minute interval over which the data are integrated.

An analysis was performed assuming a single Gaussian PAD. The derived rigidity spectra appear with similar slope. The corresponding particle flux can be adjusted on the basis of a normalization. This case results in greater residuals \mathcal{D} . Moreover, the two additional criteria for the fit goodness, namely a nearly-symmetric distribution of the residuals and relative difference between the observed and calculated NM increases to be in the order of 10–20 % is not achieved, specifically during the initial phase of the event.

Figure 7 presents the derived SEP rigidity spectra during different stages of the event, assuming a single Gaussian PAD.

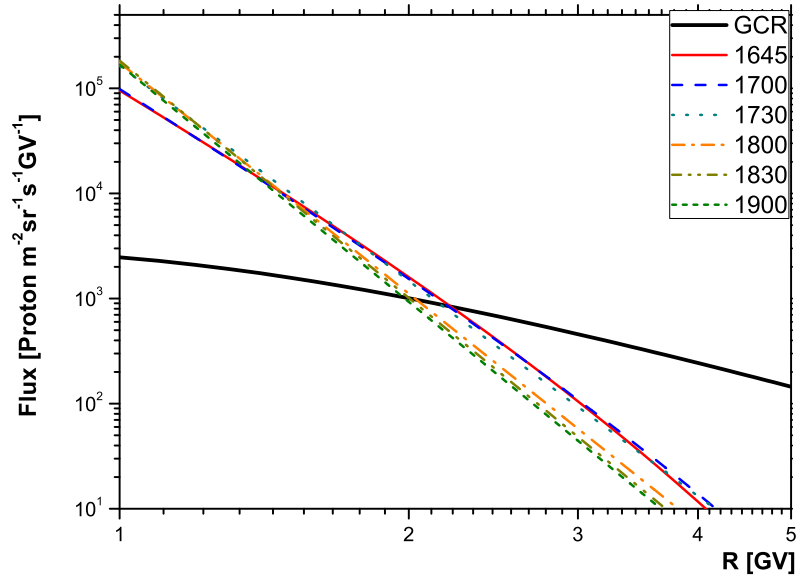


Figure 7: Derived SEP rigidity spectra during GLE 72 on 10 September 2017. The black solid line denotes the GCR particle flux, which corresponds to the time period of the GLE 72 occurrence and includes protons and α -particles, the latter representative also for heavy nuclei. Time (UT) corresponds to the start of the five minute interval over which the data are integrated.

The corresponding PADs assuming a single Gaussian are presented in Figure 8.

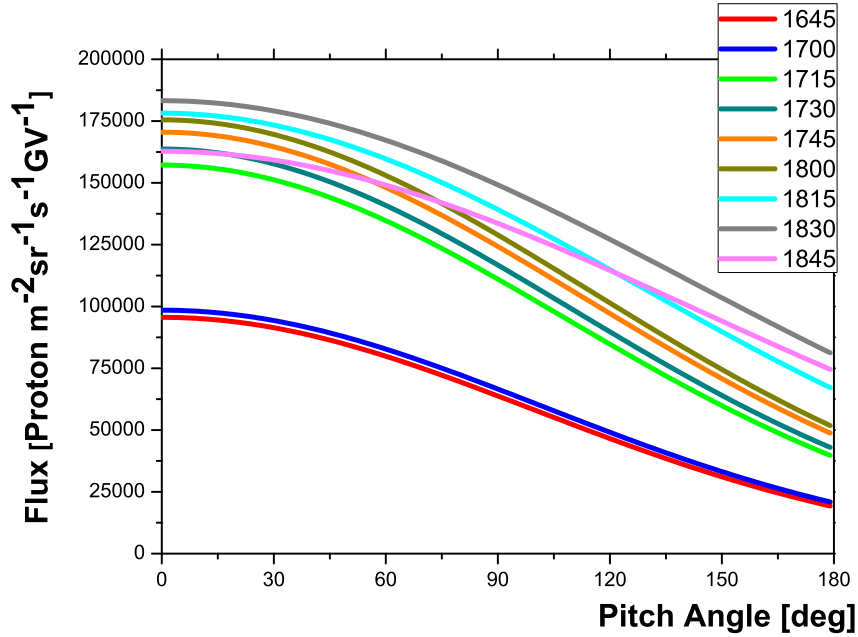


Figure 8: Derived PAD during GLE 72 on 10 September 2017. Time (UT) corresponds to the start of the five minute interval over which the data are integrated.

Finally, we tried to fit the global NM network response assuming an exponential rigidity spectrum of SEPs (Equation 2). In this case, the residual \mathcal{D} is considerably greater compared to previous cases, namely \mathcal{D} is $\approx 40\text{--}50\%$.

The accuracy of the modelling is shown by a comparison between the modelled and observed responses for several NMs during the GLE 72 on 10 September 2017 (Figure 9). Note, that the quality of the modelling is similar for the other NM stations. The comparison is performed in the case of double Gaussian PAD, while in the case of simple Gaussian the difference between modelled and experimental NM responses is considerably greater.

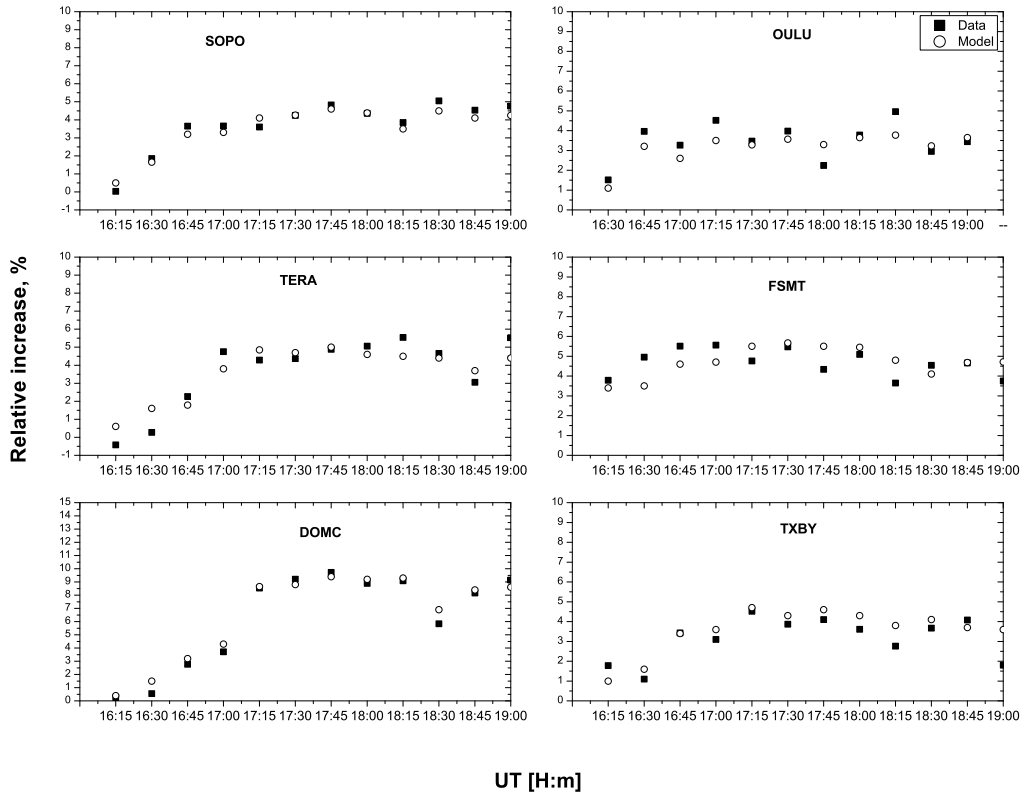


Figure 9: Modelled and observed responses of several NM stations during the GLE 72 on 10 September 2017. The accuracy of the fit for other stations is of the same order.

The particle fluence (energy, time and angle integrated particle flux) of the GLE 72 is presented in Figure 10 for the early and late phase of the event respectively. Accordingly the normalized to one hour SEP fluence is shown in Figure 11. As expected during the early phase of the event, the fluence is dominated by the high-energy part of SEPs. Accordingly during the late phase of the event the SEP flux increased at low energies.

According to our analysis the related SEPs had the Fe/O abundance ratio below 0.1 at 50-100 MeV/n (Fig.3), which is typical for gradual SEP events (e.g. Desai and Burgess, 2008; Desai and Giacalone, 2016, and references therein).

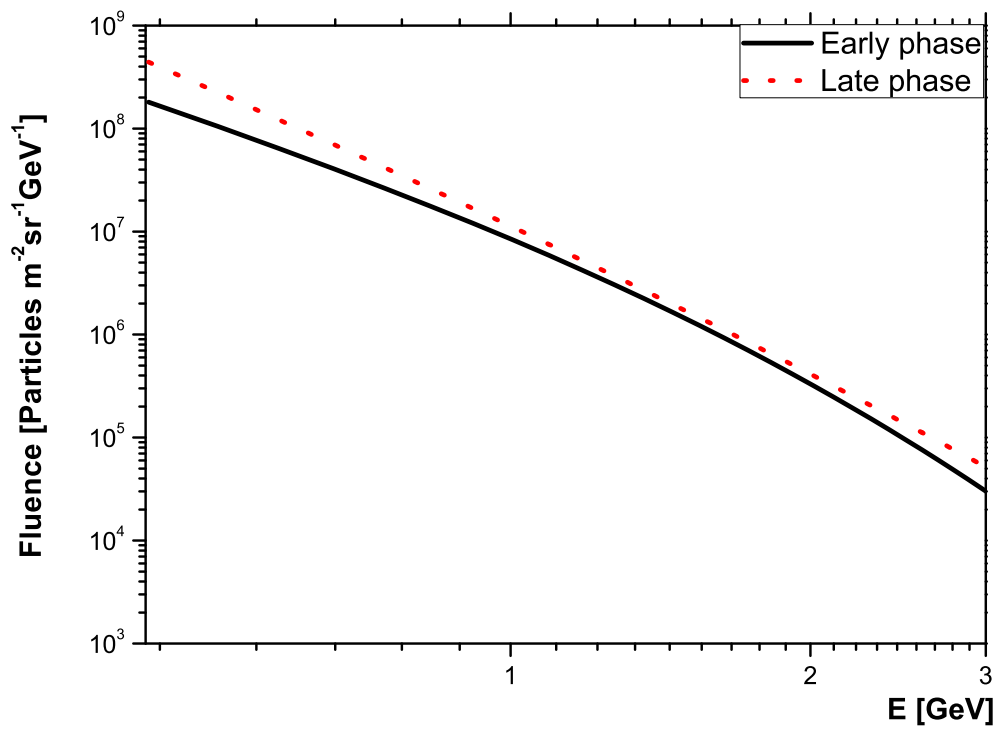


Figure 10: Fluence of high-energy SEP during GLE 72. The SEPs fluence for the early phase is angle integrated from 16:15 to 17:15 UT, while the fluence for the late phase is angle integrated from 17:15 to 19:15 UT.

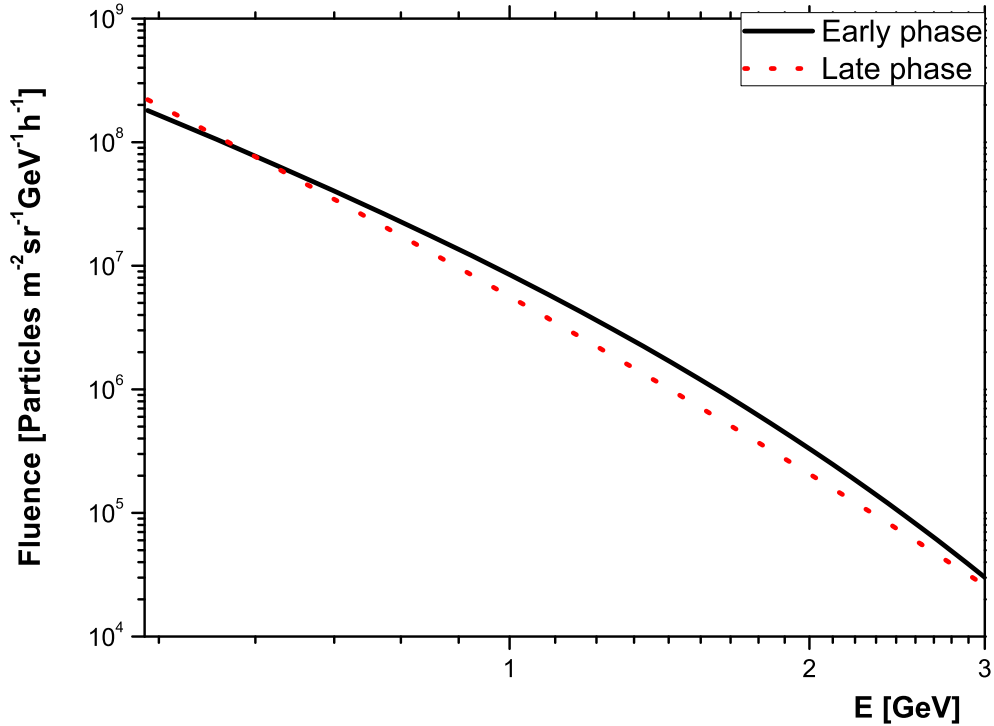


Figure 11: Normalized to 1h fluence of high-energy SEP during GLE 72 for the early and late phase of event respectively.

4 Discussion

Here we derived the spectral and anisotropy characteristics of SEPs during the weak GLE 72 event on 10 September 2017 using NM data. According to our analysis, the apparent source position was close to the direction of the IMF lines (Figure 4), the latter being estimated from the ACE satellite measurements explicitly considering the time shift of the field direction at the nose of the Earth's bow shock similarly to Mishev, Poluianov, and Usoskin (2017). According to our estimations the uncertainty of the derived apparent source position is about 10–15 degrees. This implies that particles were propagating from the Sun close to the nominal Parker spiral.

The best fit of the modelled global NM responses was achieved assuming a modified power law rigidity spectrum (Eq.1) and a wide PAD fitted with double Gaussian (Eq.3). The SEP spectrum was moderately hard during the event onset and constantly softened throughout the event. A marginal hardening was observed at about 18:15 UT. A steepening of the spectrum with rigidity, was observed during the initial phase of the event, which vanished lately. Hence, after 17:15 UT a pure power law rigidity spectrum was derived. An important anisotropy during the event onset was observed, since there were statistically significant responses at FSMT and INVK NM stations, but no or marginal at other stations. These NM stations responded to SEP fluxes with

narrow pitch angles as their asymptotic cones were close to the direction of the IMF lines (Figure 2). The angular distribution of the SEPs during the event broadened out throughout the event. The timing of the event (first increase at 16:15 with a clear shock formed already at 16:00 in the corona) is consistent with a hypothesis of particle acceleration at a coronal shock driven by the CME. In addition, the ratio Fe/O at 50–100 MeV/n is low, which is also consistent with gradual event (Desai and Burgess, 2008; Desai and Giacalone, 2016). However, a more detailed and deep analysis is necessary using all the available data in order to derive relevant information about the SEP acceleration (e.g. Kocharov *et al.*, 2017).

This derived PAD could be a result of a focused transport of SEPs with an enhanced isotropization or alternatively we can speculate that may be due to a non-standard mode of the particle propagation caused by an interplanetary magnetic field structure associated with previous CME (Ruffolo *et al.*, 2006). A detailed analysis and modelling similarly to Kocharov *et al.* (2017) is planned for forthcoming work.

5 Conclusions

Here, we have employed an improved method, compared to (Mishev, Kocharov, and Usoskin, 2014) of an analysis of data from the global neutron monitor network, namely the response of each NM is computed using a yield function corresponding to the exact NM altitude a.s.l. and self-consistent and robust optimization similarly to Mishev, Poluianov, and Usoskin (2017), applied for the GLE 72 on 10 September 2017. The data set included records from 27 NMs distributed over the globe, which encompass a wide range of the particle arrival directions and rigidities.

The method consists of consecutive computation of asymptotic directions and cut-off rigidity of the NM stations; modelling of the NM responses and solution of inverse problem. The modelling of the NMs responses is performed applying Tsyganenko 1989 and IGRF magnetospheric field models and using new NM yield function. Herein, the method employs a modified power law or exponential rigidity spectrum of SEP and superposition of two Gaussians for PAD.

We have studied several possible cases of spectral and angular distribution of SEPs, namely exponential or power law rigidity spectrum and single or double Gaussian PAD. Hence, we derived the spectral and angular characteristics of GLE particles. The time evolution of the spectral and angular characteristics is derived in the course of the event (see the supplementary materials, namely animations, which demonstrate the rigidity spectra and PAD evolution throughout the event). The 10 September 2017 event has revealed a wide PAD, best fitted with a double Gaussian, except the event onset phase, when a narrow angular distribution of SEPs is derived. The PAD parameters depict one maximum of SEP flux at/or near zero pitch angle. This is qualitatively consistent with hypothesis of focused transport (e.g. Agueda, Vainio, and Sanahuja, 2012). Fit with a single Gaussian PAD was excluded during the analysis, specifically during the initial phase of the event (16:30 UT), but the event onset with narrow PAD. The two possible fits are compared and their quality was briefly discussed.

The best fit of spectral characteristics of SEPs corresponds to a modified power law rigidity spectrum. The rigidity spectrum during the event onset is harder than that during the late phase of the event. From the derived spectra and PAD alone it is hardly possible to define an exact scenario of particle acceleration and transport, but the timing of the event as well as the derived ratio Fe/O at 50–100 MeV/n is qualitatively consistent with a shock acceleration. This study gives a basis

for subsequent studies of SEP acceleration and interplanetary transport.

Acknowledgements

This work was supported by the Academy of Finland (project No. 272157, Center of Excellence ReSoLVE and project No. 267186). Operation of the DOMC/DOMB NM was possible due to support of the French-Italian Concordia Station (IPEV program n903 and PNRA Project LTCPAA PNRA14 00091), projects CRIPA and CRIPA-X No. 304435 and Finnish Antarctic Research Program (FINNARP). We acknowledge NMDB and all the colleagues and PIs from the neutron monitor stations, who kindly provided the data used in this analysis, namely: Alma Ata, Apatity, Athens, Baksan, Dome C, Dourbes, Forth Smith, Inuvik, Irkutsk, Jang Bogo, Jungfraujoch, Kerguelen, Lomnicky Štit, Magadan, Mawson, Mexico city, Moscow, Nain, Newark, Oulu, Peawanuck, Potchefstroom, Rome, South Pole, Terre Adelie, Thule, Tixie.

References

- Aschwanden, M.: 2012, GeV particle acceleration in solar flares and ground level enhancement (GLE) events. *Space Science Reviews* **171**(1-4), 3.
- Agueda, N., Vainio, R., Sanahuja, B.: 2012, A Database of > 20 keV Electron Green's Functions of Interplanetary Transport at 1 AU. *Astrophysical Journal, Supplement Series* **202**, 18. DOI.
- Bieber, J.W., Evenson, P.A.: 1995, Spaceship Earth - an optimized network of neutron monitors. In: *Proc. of 24th ICRC Rome, Italy, 28 August - 8 September 1995* **4**, 1316.
- Bombardieri, D.J., Duldig, M.L., Michael, K.J., Humble, J.E.: 2006, Relativistic proton production during the 2000 July 14 solar event: The case for multiple source mechanisms. *Astrophysical Journal* **644**(1), 565.
- Bütikofer, R., Flückiger, E.O., Desorgher, L., Moser, M.R., Pirard, B.: 2009, The solar cosmic ray ground-level enhancements on 20 January 2005 and 13 December 2006. *Advances in Space Research* **43**(4), 499.
- Caballero-Lopez, R.A.: 2016, An estimation of the yield and response functions for the mini neutron monitor. *Journal of Geophysical Research A: Space Physics* **121**(8), 7461. DOI.
- Cliver, E.W., Kahler, S.W., Reames, D.V.: 2004, Coronal shocks and solar energetic proton events. *Astrophysical Journal* **605**, 902.
- Cooke, D.J., Humble, J.E., Shea, M.A., Smart, D.F., Lund, N., Rasmussen, I.L., Byrnek, B., Goret, P., Petrou, N.: 1991, On cosmic-ray cutoff terminology. *Il Nuovo Cimento C* **14**(3), 213.
- Cramp, J.L., Humble, J.E., Duldig, M.L.: 1995, The cosmic ray ground-level enhancement of 24 October 1989. In: *Proceedings Astronomical Society of Australia* **11**, 28.
- Cramp, J.L., Duldig, M.L., Flückiger, E.O., Humble, J.E., Shea, M.A., Smart, D.F.: 1997, The October 22, 1989, solar cosmic enhancement: ray an analysis the anisotropy spectral characteristics. *Journal of Geophysical Research* **102**(A11), 24 237.
- Debrunner, H., Flückiger, E.O., Gradel, H., Lockwood, J.A., McGuire, R.E.: 1988, Observations related to the acceleration, injection, and interplanetary propagation of energetic protons during the solar cosmic ray event on February 16, 1984. *Journal of Geophysical Research* **93**(A7), 7206.
- Dennis, J.E., Schnabel, R.B.: 1996, *Numerical methods for unconstrained optimization and non-linear equations*, Prentice-Hall, Englewood Cliffs. ISBN 13-978-0-898713-64-0.
- Desai, M., Giacalone, J.: 2016, Large gradual solar energetic particle events. *Living Reviews in Solar Physics* **13**(1), 3. DOI.
- Desai, M.I., Burgess, D.: 2008, Particle acceleration at coronal mass ejection driven interplanetary shocks and the earth's bow shock. *Journal of Geophysical Research: Space Physics* **113**(A9), A00B006. DOI.

- Desorgher, L., Flückiger, E.O., Gurtner, M., Moser, M.R., Bütikofer, R.: 2005, A Geant 4 code for computing the interaction of cosmic rays with the earth's atmosphere. *International Journal of Modern Physics A* **20**(A11), 6802.
- Drake, J.F., Cassak, P.A., Shay, M.A., Swisdak, M., Quataert, E.: 2009, A magnetic reconnection mechanism for ion acceleration and abundance enhancements in impulsive flares. *Astrophysical Journal* **700**(1 PART 2), L16. DOI.
- Gil, A., Usoskin, I.G., Kovaltsov, G.A., Mishev, A.L., Corti, C., Bindi, V.: 2015, Can we properly model the neutron monitor count rate? *J. Geophys. Res.* **120**, 7172.
- Gopalswamy, N., Xie, H., Yashiro, S., Akiyama, S., Mäkelä, P., Usoskin, I.G.: 2012, Properties of ground level enhancement events and the associated solar eruptions during solar cycle 23. *Space Science Reviews* **171**(1-4), 23.
- Gopalswamy, N., Xie, H., Akiyama, S., Mkel, P.A., Yashiro, S.: 2014, Major solar eruptions and high-energy particle events during solar cycle 24. *Earth, Planets and Space* **66**(1), 104. cited By 32. DOI.
- Hatton, C.: 1971, The neutron monitor. In: *Progress in Elementary Particle and Cosmic-ray Physics X*, North Holland Publishing Co., Amsterdam. Chap. 1.
- Himmelblau, D.M.: 1972, *Applied nonlinear programming*, Mcgraw-Hill(Tx), ISBN 978-0070289215.
- Humble, J.E., Duldig, M.L., Smart, D.F., Shea, M.A.: 1991, Detection of 0.5–15 GeV solar protons on 29 September 1989 at australian stations. *Geophysical Research Letters* **18**(4), 737.
- Kallenrode, M.-B., Cliver, E.W., Wibberenz, G.: 1992, Composition and azimuthal spread of solar energetic particles from impulsive and gradual flares. *Astrophysical Journal* **391**(1), 370.
- Kocharov, L., Pohjolainen, S., Mishev, A., Reiner, M.J., Lee, J., Laitinen, T., Didkovsky, L.V., Pizzo, V.J., Kim, R., Klassen, A., Karlicky, M., Cho, K.-S., Gary, D.E., Usoskin, I., Valtonen, E., Vainio, R.: 2017, Investigating the origins of two extreme solar particle events: Proton source profile and associated electromagnetic emissions. *Astrophysical Journal* **839**(2), 79.
- Kudela, K., Usoskin, I.: 2004, On magnetospheric transmissivity of cosmic rays. *Czechoslovak Journal of Physics* **54**(2), 239.
- Kudela, K., Bučik, R., Bobik, P.: 2008, On transmissivity of low energy cosmic rays in disturbed magnetosphere. *Advances in Space Research* **42**(7), 1300.
- Langel, R.A.: 1987, Main field in geomagnetism. In: *Geomagnetism*, J.A. Jacobs Academic Press, London, 249. Chap. 1.
- Lara, A., Borgazzi, A., Caballero-Lopez, R.: 2016, Altitude survey of the galactic cosmic ray flux with a mini neutron monitor. *Advances in Space Research* **58**(7), 1441. DOI.
- Levenberg, K.: 1944, A method for the solution of certain non-linear problems in least squares. *Quarterly of Applied Mathematics* **2**, 164.

- Li, G., Moore, R., Mewaldt, R.A., Zhao, L., Labrador, A.W.: 2012, A twin-CME scenario for ground level enhancement events. *Space Science Reviews* **171**(1-4), 141.
- Lockwood, J.A., Debrunner, H., Flückiger, E.O.: 1990, Indications for diffusive coronal shock acceleration of protons in selected solar cosmic ray events. *Journal of Geophysical Research: Space Physics* **95**(A4), 4187.
- Mangeard, P.-S., Ruffolo, D., Siz, A., Nuntiyakul, W., Bieber, J.W., Clem, J., Evenson, P., Pyle, R., Duldig, M.L., Humble, J.E.: 2016, Dependence of the neutron monitor count rate and time delay distribution on the rigidity spectrum of primary cosmic rays. *Journal of Geophysical Research: Space Physics* **121**(12), 11,620. DOI.
- Marquardt, D.: 1963, An algorithm for least-squares estimation of nonlinear parameters. *SIAM Journal on Applied Mathematics* **11**(2), 431.
- Mavrodiev, S.C., Mishev, A.L., Stamenov, J.N.: 2004, A method for energy estimation and mass composition determination of primary cosmic rays at the chacaltaya observation level based on the atmospheric cherenkov light technique. *Nuclear Instruments and Methods in Physics Research, Section A: Accelerators, Spectrometers, Detectors and Associated Equipment* **530**(3), 359. DOI.
- Mavromichalaki, H., Papaioannou, A., Plainaki, C., Sarlanis, C., Souvatzoglou, G., Gerontidou, M., Papailiou, M., Eroshenko, E., Belov, A., Yanke, V., Flückiger, E.O., Bütikofer, R., Parisi, M., Storini, M., Klein, K.-L., Fuller, N., Steigies, C.T., Rother, O.M., Heber, B., Wimmer-Schweingruber, R.F., Kudela, K., Strharsky, I., Langer, R., Usoskin, I., Ibragimov, A., Chilingaryan, A., Hovsepyan, G., Reymers, A., Yeghikyan, A., Kryakunova, O., Dryn, E., Nikolayevskiy, N., Dorman, L., Pustil'Nik, L.: 2011, Applications and usage of the real-time neutron monitor database. *Advances of Space Research* **47**, 2210.
- Mishev, A., Usoskin, I.: 2016a, Analysis of the ground level enhancements on 14 July 2000 and on 13 December 2006 using neutron monitor data. *Solar Physics* **291**(4), 1225.
- Mishev, A., Usoskin, I.: 2016b, Erratum to: analysis of the ground level enhancements on 14 July 2000 and on 13 December 2006 using neutron monitor data. *Solar Physics* **291**(4), 1579.
- Mishev, A.L., Kocharov, L.G., Usoskin, I.G.: 2014, Analysis of the ground level enhancement on 17 May 2012 using data from the global neutron monitor network. *Journal of Geophysical Research* **119**, 670.
- Mishev, A., Poluianov, S., Usoskin, I.: 2017, Assessment of spectral and angular characteristics of sub-geomagnetic events using the global neutron monitor network. *Journal of Space Weather and Space Climate* **7**, A28. DOI.
- Mishev, A., Usoskin, I., Kocharov, L.: 2017, Using global neutron monitor network data for geomagnetic event analysis: recent results. *Proceedings of Science, Proc. of 35th ICRC Busan, Korea, 12 - 20 July 2017*, 147.
- Mishev, A., Usoskin, I., Kovaltsov, G.: 2013, Neutron monitor yield function: New improved computations. *Journal of Geophysical Research* **118**, 2783.

- Mishev, A., Usoskin, I., Kovaltsov, G.: 2015, New neutron monitor yield function computed at several altitudes above the sea level: Application for GLE analysis. *Proceedings of Science, Proc. of 34th ICRC Hague, Netherlands, 30 July - 6 August 2015*, 159.
- Moraal, H., McCracken, K.G.: 2012, The time structure of ground level enhancements in solar cycle 23. *Space Science Reviews* **171**(1-4), 85.
- Nevalainen, J., Usoskin, I., Mishev, A.: 2013, Eccentric dipole approximation of the geomagnetic field: Application to cosmic ray computations. *Advances in Space Research* **52**(1), 22.
- Papaioannou, A., Souvatzoglou, G., Paschalis, P., Gerontidou, M., Mavromichalaki, H.: 2014, The first ground-level enhancement of solar cycle 24 on 17 May 2012 and its real-time detection. *Solar Physics* **289**(1), 423. DOI.
- Reames, D.V.: 1999, Particle acceleration at the sun and in the heliosphere. *Space Science Reviews* **90**(3-4), 413.
- Reames, D.V.: 2013, The two sources of solar energetic particles. *Space Science Reviews* **175**(1-4), 53. DOI.
- Ruffolo, D., Tooprakai, P., Rujiwarodom, M., Khumlumlert, T., Wechakama, M., Bieber, J.W., Evenson, P.A., Pyle, K.R.: 2006, Relativistic solar protons on 1989 October 22: Injection and transport along both legs of a closed interplanetary magnetic loop. *Astrophysical Journal* **639**(2), 1186.
- Shea, M.A., Smart, D.F.: 1982, Possible evidence for a rigidity-dependent release of relativistic protons from the solar corona. *Space Science Reviews* **32**, 251.
- Shea, M.A., Smart, D.F.: 1990, A summary of major solar proton events. *Solar Physics* **127**, 297.
- Simpson, J., Fonger, W., Treiman, S.: 1953, Cosmic radiation intensity-time variation and their origin. i. neutron intensity variation method and meteorological factors. *Physical Review* **90**, 934.
- Souvatzoglou, G., Papaioannou, A., Mavromichalaki, H., Dimitroulakos, J., Sarlanis, C.: 2014, Optimizing the real-time ground level enhancement alert system based on neutronmonitor measurements: Introducing gle alert plus. *Space Weather* **12**(11), 633. DOI.
- Stoker, P.H., Dorman, L.I., Clem, J.M.: 2000, Neutron monitor design improvements. *Space Science Reviews* **93**(1-2), 361.
- Tikhonov, A.N., Goncharsky, A.V., Stepanov, V.V., Yagola, A.G.: 1995, *Numerical methods for solving ill-posed problems*, Kluwer Academic Publishers, Dordrecht. ISBN 978-90-481-4583-6.
- Tsyganenko, N.A.: 1989, A magnetospheric magnetic field model with a warped tail current sheet. *Planetary and Space Science* **37**(1), 5.

- Tylka, A., Dietrich, W.: 2009, A new and comprehensive analysis of proton spectra in ground-level enhanced (GLE) solar particle events. In: *Proc. of 31th ICRC Lodz, Poland, 7 -15 July 2009*, 0273.
- Vainio, R., Valtonen, E., Heber, B., Malandraki, O.E., Papaioannou, A., Klein, K.-L., Afanasiev, A., Agueda, N., Aurass, H., Battarbee, M., Braune, S., Dröge, W., Ganse, U., Hamadache, C., Heynderickx, D., Huttunen-Heikinmaa, K., Kiener, J., Kilian, P., Kopp, A., Kouloumvakos, A., Maisala, S., Mishev, A., Miteva, R., Nindos, A., Oittinen, T., Raukunen, O., Riihonen, E., Rodriguez-Gasn, R., Saloniemi, O., Sanahuja, B., Scherer, R., Spanier, F., Tatischeff, V., Tziotziou, K., Usoskin, I.G., Vilmer, N.: 2013, The first SEPserver event catalogue 68-MeV solar proton events observed at 1 au in 1996-2010. *Journal of Space Weather and Space Climate* **3**, A12. DOI.
- Vainio, R., Raukunen, O., Tylka, A.J., Dietrich, W.F., Afanasiev, A.: 2017, Why is solar cycle 24 an inefficient producer of high-energy particle events? *Astronomy and Astrophysics* **604**, A47. DOI.
- Vashenyuk, E.V., Balabin, Y.V., Perez-Peraza, J., Gallegos-Cruz, A., Miroshnichenko, L.I.: 2006, Some features of the sources of relativistic particles at the sun in the solar cycles 21-23. *Advances Space Research* **38**(3), 411.
- Vashenyuk, E.V., Balabin, Y.V., Gvozdevsky, B.B., Schur, L.I.: 2008, Characteristics of relativistic solar cosmic rays during the event of December 13, 2006. *Geomagnetism and Aeronomy* **48**(2), 149.